Code Surrogate Development for Dynamic PRA Using Anisotropic Taylor Kriging Methodology

Robby Christian[1], Hyun Gook Kang[2]
[1,2]Rensselaer Polytechnic Institute, Troy, USA

Abstract: An inherent challenge in Dynamic Probabilistic Risk Assessment methodologies is on managing the large number of dynamic scenarios to be investigated. This paper proposes an interpolation-based code surrogate methodology to resolve this challenge. It adopted the Shape Dynamic Time Warping algorithm to cluster the interpolation neighborhood from time series sample data. The interpolation method was adapted from Taylor Kriging, with an extension to allow a Reduced-Order Model of the Taylor series. The proposed methodology was applied to generate risk response surfaces to estimate Emergency Core Cooling System (ECCS) criteria for SiC Accident Tolerant Fuel concept. The response surface was exploited to estimate the cumulative failure probability of SiC cladding due to the uncertainty in active Safety Injection actuation timing.

Keywords: Dynamic PRA, Code Surrogate, Accident Tolerant Fuel.

1. INTRODUCTION

Probabilistic Risk Assessment (PRA) provides a systematic method to quantify risk probabilistically through the use of Event Trees (ETs) and Fault Trees (FTs). In doing so, it adopts the Boolean classification method to assign the status of branches in ET and FT. A component is classified as successful or failed based on its capability to perform its intended function independent from the system's parameters. This approach provides a simple way to present the root-causes of an event in the form of cutsets. However, it is not suitable for dynamic systems, i.e. systems which responses to initial perturbations evolve over time as system components interact with each other and with the environment [1].

Risk of dynamic systems can be more adequately quantified by using the Dynamic PRA (DPRA) methodology. DPRA recognizes that component uncertainties may alter the system's response which in turn affects the success probability of other components. These uncertainties may lead to a large number of scenarios for a single initiating event, making them difficult to incorporate in the classical PRA model [2]. Current solutions to this challenge are creation of scenario clusters [2] and process surrogates [3]. This research focuses on the development of a process surrogate for dynamic risk assessment. This methodology is then implemented to analyze the performance of Accident Tolerant Fuel (ATF) due to a Loss-of-Coolant-Accident (LOCA) in nuclear power plants (NPPs). The following sub-section describe the risk assessment framework to provide a background for the code surrogate derivation.

1.1. Probabilistic Risk Assessment on Accident Tolerant Fuel (ATF)

1.1.1. Dynamic Risk Measure of Silicon-Carbide ATF

U.S. Nuclear Regulatory Commision (NRC) has introduced a performance-based safety requirement in a draft regulation [4] for Light Water Reactor (LWR) NPPs. Contrary to the current prescriptive-based regulation, this draft requires NPP utilities to evaluate Emergency Core Cooling System (ECCS) performance during a Loss-of-Coolant-Accident (LOCA) realistically by considering uncertainties. With all the possible LOCA scenarios, the fuel performance requirements must be satisfied, i.e. the fuel must maintain a coolable geometry, does not generate hydrogen more than a certain limit, and amenable to the long-term cooling.

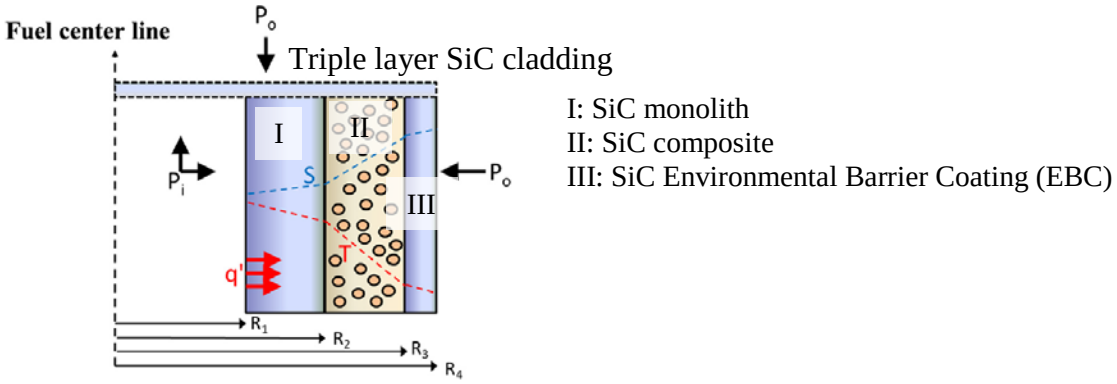

Figure 1. Triple layer Silicon-Carbide nuclear fuel cladding

In this research, we evaluated these requirements on ATF as an emerging nuclear fuel concept after the Fukushima Dai-ichi nuclear plant accident [5]. We focused our scope to triple layer Silicon-Carbide (SiC) type ATF [6] as shown in Figure 1, which is one of the best ATF candidate considered to replace the current Zirconium-based fuel. Although SiC has a reduced oxidation rate and a higher melting temperature than Zircalloy-4 cladding, it is prone to thermal shocks due to the quenching of hot fuel rods with cold water. In LOCA case, this quenching happens when ECCS safety injection refloods the core after fuel rods are uncovered with water. The stress distribution S due to differential pressure and temperature loading is illustrated in Figure 1. This mechanical stress can induce cracks, which may statistically cause the SiC cladding to fail following a Weibull distribution. It was conservatively assumed that cracks in the innermost and outermost CVD-SiC layer lead to the failure of fission product retention. In this assumption, no credit is given to the SiC fiber composite layer to retain fission gas. Layer I and II function as load bearing structure, and therefore their failure indicates a failure to maintain fuel rod's coolable geometry. Clad catastrophic failure happens when all three layers fail altogether.
The current ECCS criteria place a deterministic limit on the peak cladding temperature and equivalent cladding reacted. However, the stochastic nature of SiC cladding failure implies that any variation in ECCS actuation may cause cladding failure. For that reason, the cladding failure probability was integrated over the range of ECCS operational uncertainty as illustrated in Figure 2. Integrating a vertical cut at the failure distribution response surface provides the cladding failure probability at a certain time, due to uncertainty of ECCS and thermal hydraulic parameters. Meanwhile, an integration of a horizontal cut implies total clad failure probability within a bounded time window due to thermal hydraulic parameters exceeding a setpoint as given in Equation (1). The setpoint is selected as the ECCS criteria when the integral equals to the failure probability of current Zr-based clad LBLOCA, which indicates that the selected configuration fails to improve safety.

$$P_{fail} = \int_{SP1}^{\infty} \left(\int p \; dt \right) dTH \tag{1}$$

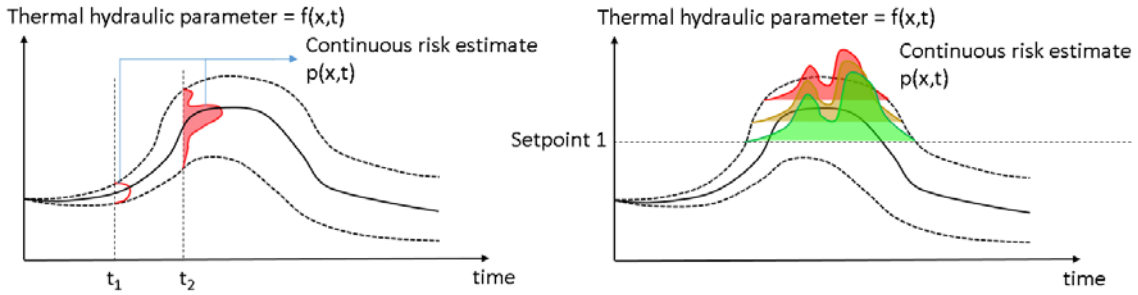

Figure 2. Estimation of ECCS criteria for a stochastic clad failure

1.1.2. Code Surrogate For Accident Tolerant Fuel PRA

The reactor's system parameter during steady-state operation and accident was estimated using RELAP5-3D. In this work, we use the model of a 1000 MWe Pressurized Water Reactor (PWR) NPP.

The major components of the model include the reactor core, 2 hot-legs, 2 steam generators, 2 feedwater systems, 4 redundant ECCS channels, and a pressurizer. Its ECCS comprises of passive (SIT), active high pressure (HPSI) and active low pressure (LPSI) injection system.

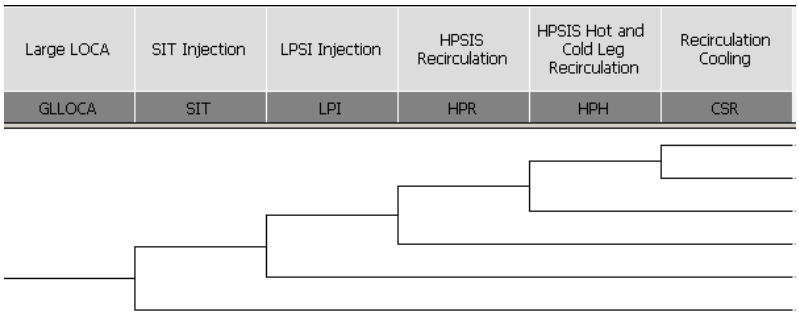

Figure 3. LBLOCA mitigation event tree

The safety functions required to mitigate LBLOCA are shown in Figure 3. Dynamic uncertainties of active safety injection were sampled for simulations in RELAP5. Clad temperature distribution, thermomechanical stress and the corresponding clad failure probability were estimated using the methodologies described in reference [6]. The code surrogate was built to refine the failure probability response surface from sampled simulations, in order to provide a more accurate integration result of equation (1).

2. METHODOLOGY

Results of reactor safety analysis code are presented as time series. Variations in active SI actuation timing cause variation in the timing and extent of thermal shock events between sampled time series. To interpolate results between two time series, it is required to estimate the time shift from similar physics. This is done by utilizing Shape Dynamic Time Warping (SDTW). After the interpolation neighborhood have been identified, the interpolation value is estimated with Taylor Kriging (TK) methodology.

2.1. Shape Dynamic Time Warping (SDTW)

SDTW [7] is a variant of the Dynamic Time Warping (DTW) algorithm to match features on two time series datasets. Contrary to DTW, SDTW attempts to achieve locally sensible matchings while maintaining a global optimal solution. It works by encoding local structures by their shape descriptors, and matches these descriptors by using DTW algorithm, as illustrated in Figure 4. Results of SDTW algorithm is a matrix of time steps from the code runs to be included in the interpolation neighborhood.

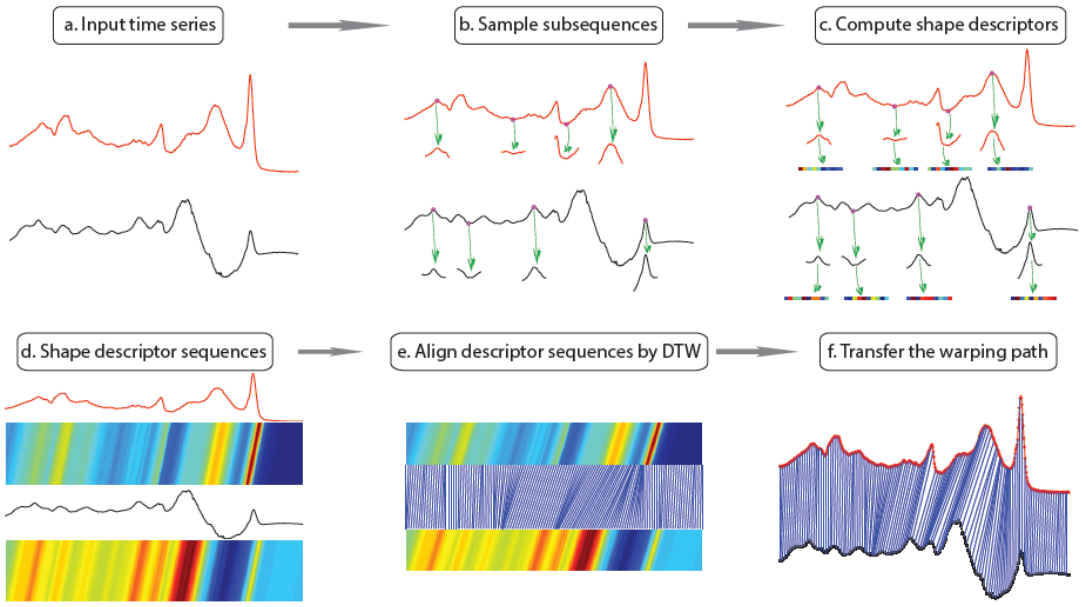

Figure 4. Shape DTW algorithm [7]

2.2. Taylor Kriging

The code surrogate will be adapted from existing interpolation method, i.e. Taylor Kriging (TK) [8] [9] based on the following considerations:

1. TK is an unbiased estimator, i.e. does not consistently under or over predict.
2. TK provides an uncertainty estimate to its prediction
3. TK can be used to estimate non-linear trend among sample data
4. In the process of building a TK-based code surrogate model, vectors of derivatives were estimated from sample data to determine the order of Taylor series. These derivative vectors serve two additional valuable purposes as follows:
   a. To cluster the interpolation vector based on the continuity of physical process among samples. A discontinuity in nuclear plant safety analysis may be caused by an abrupt transition of heat transfer mode between sampled scenarios. These situations, as illustrated in Figure 5, can be detected by monitoring the continuity of derivative vectors.
   b. To provide insights on the sensitivity of each uncertainty source to the predicted variable and to the final risk measure.

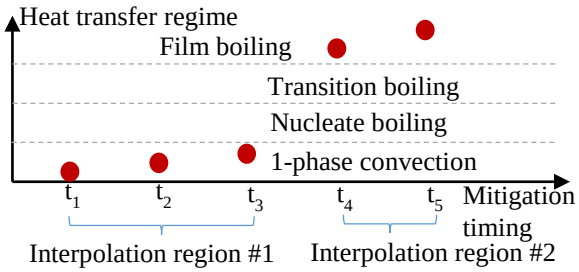

Figure 5. Illustration on discontinuity of physical process between samples in nuclear plant accident mitigation

TK response function comprises of a regression and stochastic term as illustrated in Figure 6 Its regression term m(x) is in the form of a Taylor series expansion, hence its name Taylor Kriging. TK was developed and tested on explicit mathematical functions [8] where the m(x) term had a finite series' order and could be estimated with a simple finite difference approach. This condition however is different in complex dynamic code simulations. Complex codes have epistemic uncertainties due to limited knowledge on the modelled physical process. These immeasurable uncertainties are presented for example as empirical correlations used to calculate heat transfer coefficients for various heat transfer modes in RELAP5. These uncertainties can introduce approximation errors, or "noise", to sampled data [10]. The noise may cause the Taylor series expansion in m(x) to be of high or infinite order, which makes TK challenging to solve.

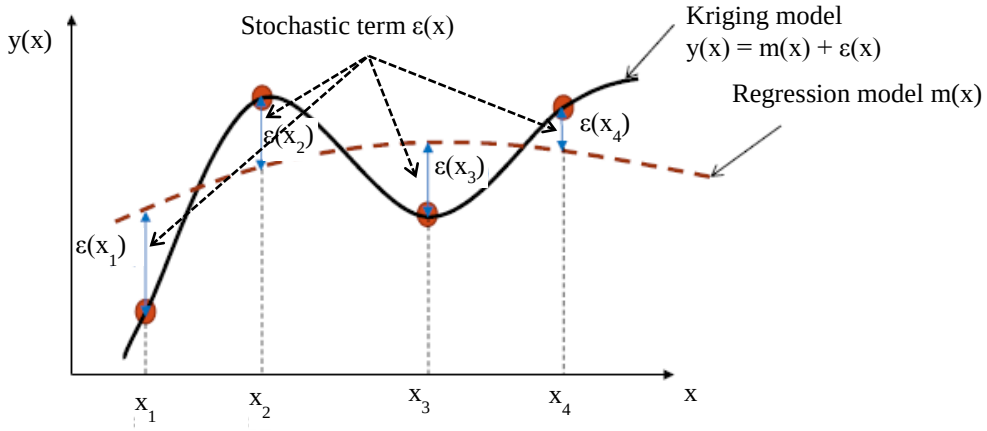

Figure 6. Illustration of TK response function

To overcome the aforementioned challenge, we attempt to fit a reduced-order regression term m(x) and estimate the corresponding TK uncertainty. We modify the original TK formulation to include error

terms due to the reduction of m(x) to a lower order Taylor series. Let the Taylor series approximation $\hat{m}(x)$ to the regression function m(x) be formulated as:

$$\hat{m}(x) = \sum_{i=0}^{M} \frac{m^{(i)}(x_0)}{i!}(x - x_0)^i + \sum_{j=M+1}^{N} \frac{m^{(j)}(x_0)}{j!}(x - x_0)^j \quad (2)$$

Where x_0 is the Taylor expansion point, (i) and (j) indicates the i-th and j-th derivative. If we approximate to a reduced order M < N, there will be a disparity between the M^{th} order derivative of $\hat{m}$, and of m at x_0:

$$\hat{m}^{(M)}(x) = m^{(M)}(x_0) + E(x) = m^{(M)}(x_0) + \sum_{j=1}^{N-M} \frac{m^{(M+j)}(x_0)}{j!}(x - x_0)^j \quad (3)$$

This disparity is illustrated in Figure 7a. Based on the Taylor expansion theorem, the error from this Taylor order reduction has a ceiling of the Lagrange Error Bound (LEB) given in Equation 4, which is illustrated in Figure 7b.

$$E_{M+1} \le LEB, \qquad LEB = \frac{\mu}{(M+1)!}(x - x_0)^{M+1}, \qquad \mu = \max\left|\hat{m}^{(M+1)}(x)\right| \quad (4)$$

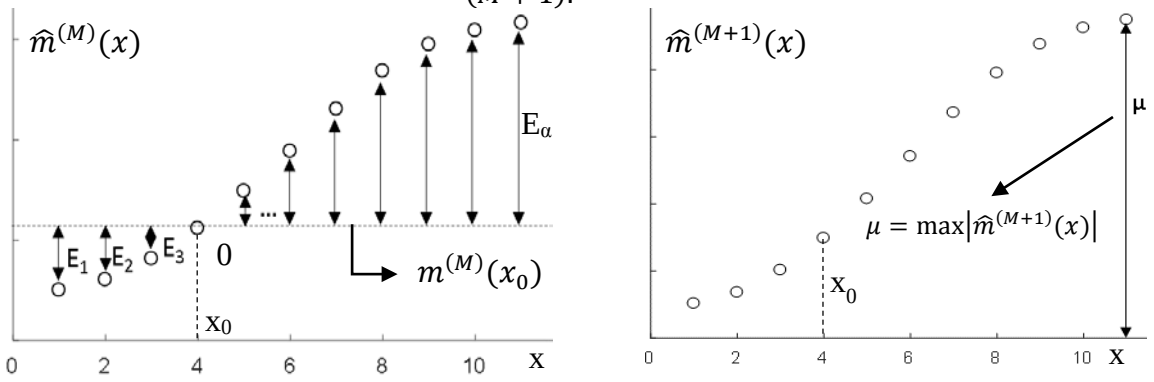

(a) Taylor-series reduced-order error

(b) Maximum value on $(M+1)^{th}$ derivative to estimate LEB

Figure 7. Error caused by the reduction of Taylor series' order

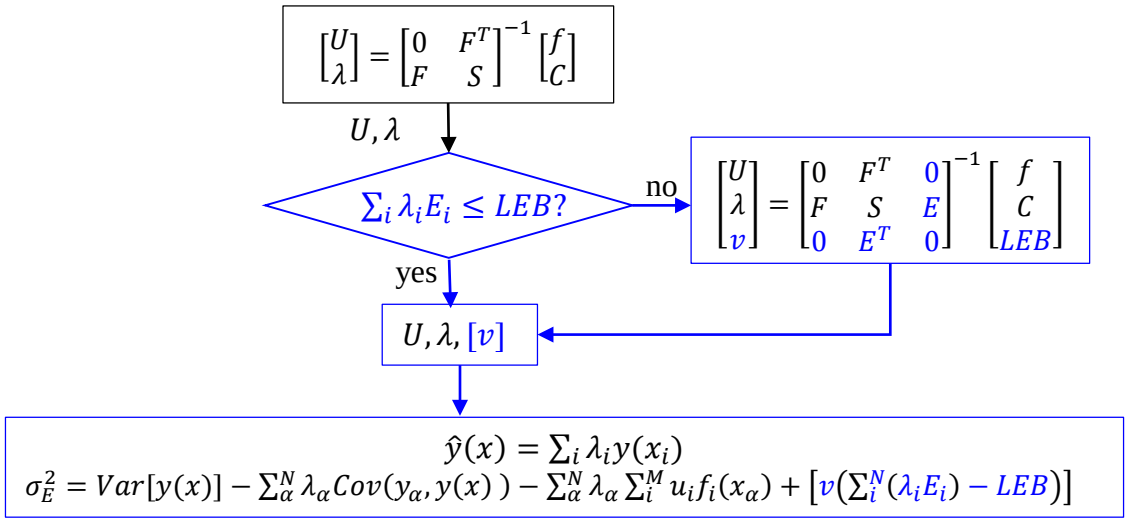

Figure 8. Modified TK formulation

By introducing equation 3 and 4 into the analytical derivation of TK [8], TK becomes a problem of constrained optimization with a Karush-Kuhn-Tucker condition [11], which we solve using the flowchart in Figure 8. In this figure, the blue boxes are our new contributions to the previous TK formulation, $\hat{y}(x)$ and σ_E^2 are TK estimate and error variance respectively, i indicates sampled data, x_i is sample points, λ is the vector of interpolation weighting factor applied to neighboring data, E^T is a

column vector of $[E_1(x_1-x_0)^M, \ldots, E_i(x_i-x_0)^M]/M!$ taken from Figure 7a, and v is the Lagrange multiplier for the inequality in Equation 4.

3. RESULTS AND DISCUSSIONS

Figure 9 shows the initial temperature and stress distribution within the cladding of the hottest fuel rod when LBLOCA accident occurs. Mechanical stress due to the temperature and differential pressure loadings shown in this figure were used to estimate the failure probability of each SiC clad layer. Clad failure modes were estimated from the combined failure probability of these individual layers.

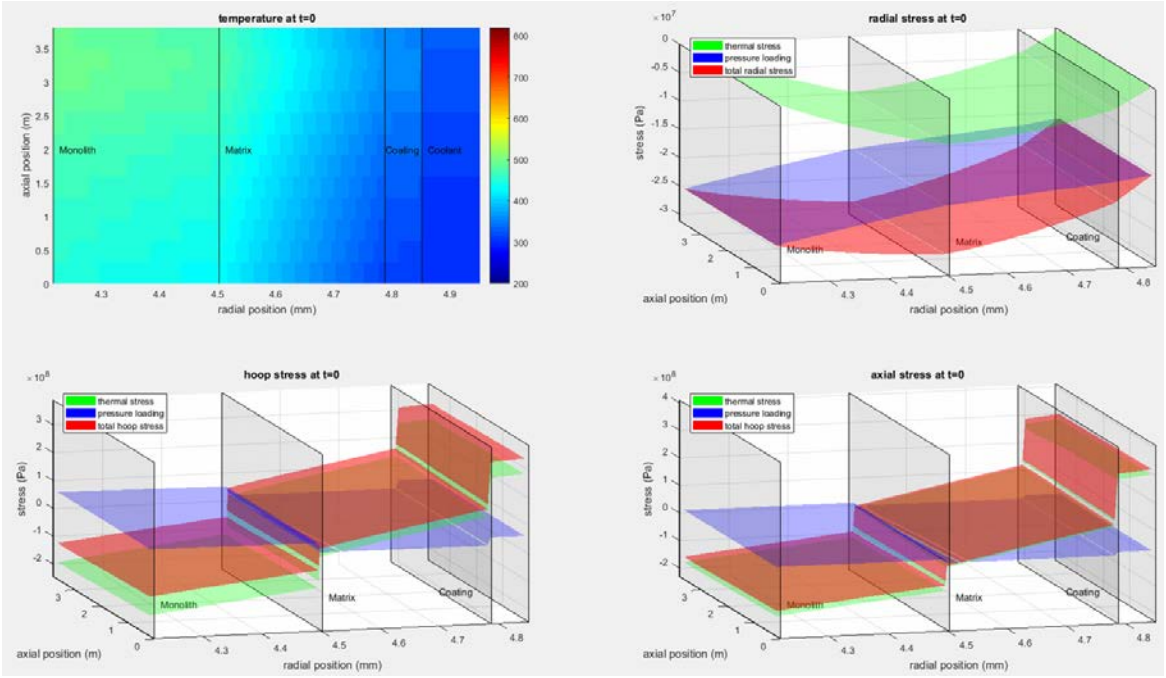

Figure 9. Clockwise direction from the top left: Temperature distribution, radial stress, axial stress and hoop stress within SiC cladding at steady-state operation

Figure 10 shows the probability of various modes of clad failure when core was reflooded within about 30 seconds after a LBLOCA initiating event. This reflood timing is the current delay time to effectively remove decay heat from fuel rods with current Zr cladding [12] [13]. Subsequent quenching of the hot cladding surface by the passive safety injection tank (SIT) at t=14 s followed by active SI injection at t=32 s contributed to the steep jumps in clad failure probability. The figure shows that the clad's fission product retention capability had the highest failure probability. Therefore, this failure mode was selected as the limiting factor to determine ECCS criteria.

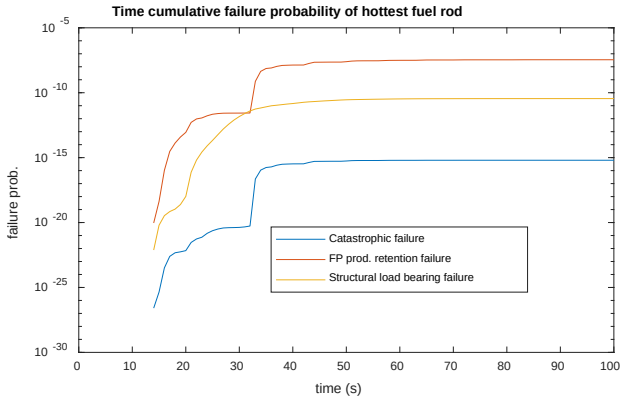

Figure 10. SiC clad failure probability

Active SI injection delay was further varied from zero to 150 seconds with a sampling interval of 15 seconds. The Peak Cladding Temperature (PCT) due to this variation is shown in Figure 11. The clad did not melt and fail deterministically even at the maximum active SI delay in this study. However, it may fail stochastically with a certain probability at any given time step as shown in Figure 12. The figure suggests that early actuation of active SI injection may be undesirable because it increases the extent of thermomechanical stress and clad failure. In order to find the upper limit of the active SI injection delay, a double integration of the response surface in Figure 12 is required. A finer sampling interval may give a better integral, at the expense of an increased computational cost. The proposed code surrogate may give an estimate of this integral without this downside.

Figure 13 shows the connection between data points in Figure 12 as estimated by SDTW algorithm. This data selection is a pre-requisite to create a surrogate using TK interpolation. However, it also informs of several physical insights. There were no time shifts observed when active SI delay was beyond 90 seconds. It was because the nominal failure probabilities were similar, as shown in Figure 12. It might be because most thermomechanical shock events occurred during SIT injection which lasted until $t \approx 80$ seconds. The second observation is that time shift started to occur around $t = 30$ seconds. This might be because the blowdown phase was completed and core level started to rise around $t = 30$ seconds, starting from which a significant difference in heat removal rate and thermomechanical stress started to take place between the different scenarios.

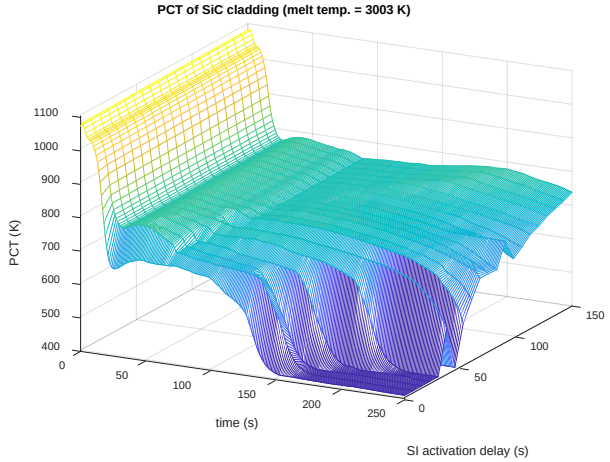

Figure 11. Peak Cladding Temperature (PCT) of SiC cladding

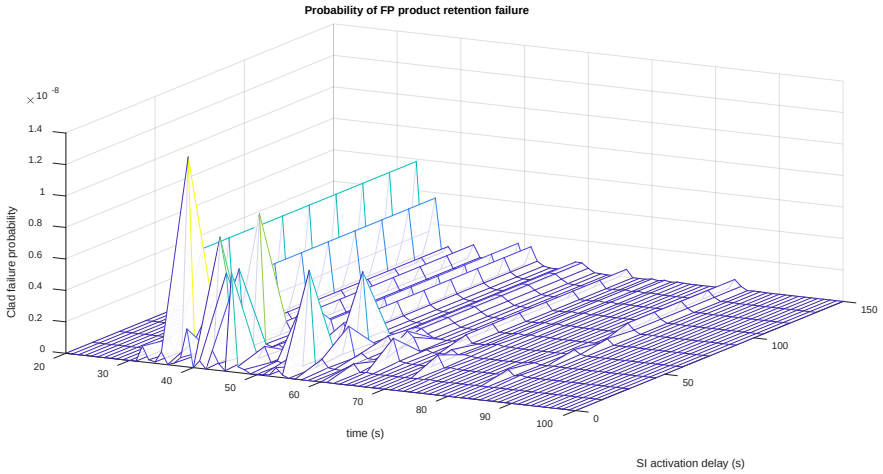

Figure 12. Probability of fission product retention failure with SiC cladding

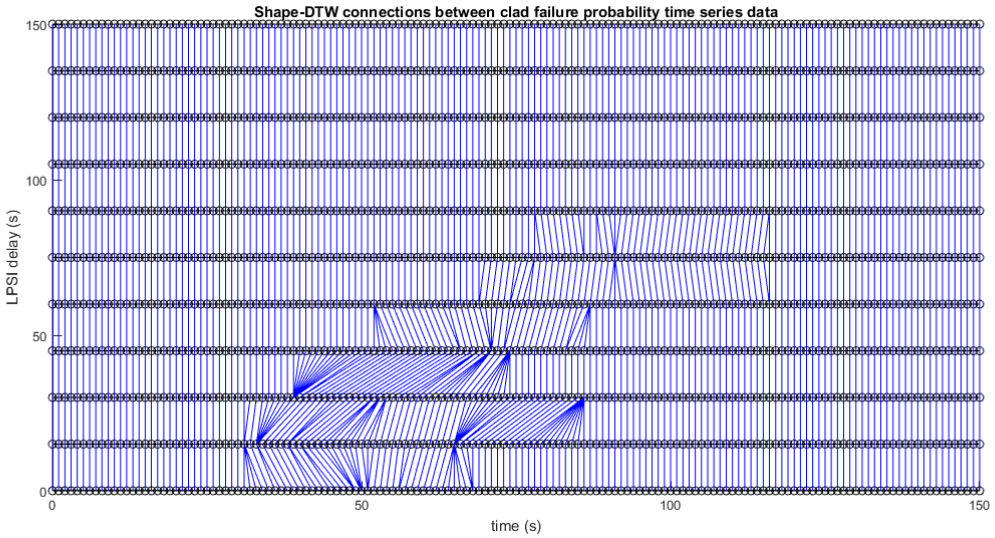

Figure 13. SDTW connections between clad failure probabilities shown in Figure 12

Figure 14 compares the integral results when the SI delay was sampled every 15 seconds (coarse mesh) and when the mesh resolution was doubled. The figure expresses the clad failure probability before a certain time step because of a uniform uncertainty distribution of SI delay up to 150 seconds. The increase in mesh resolution improved the integral result by 8 %, and the difference between integral from code surrogate and the true value was 0.7 %. Research is underway to investigate a prolonged SI delay in the case of an extended station blackout. Further results will be presented at the conference.

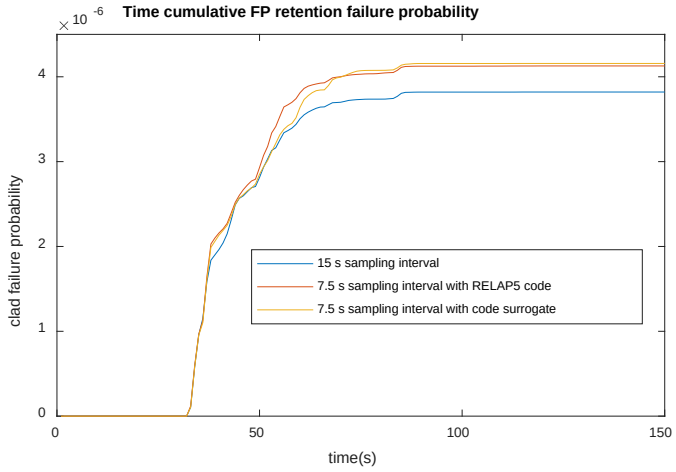

Figure 14. Cumulative probability of fission product retention failure due to uncertainty of active SI injection delay between 0 and 150 seconds

4. CONCLUSION

A code surrogate methodology for dynamic PRA application was developed based on the Shape Dynamic Time Warping and Taylor Kriging algorithm. The methodology was aimed at generating a full-rank risk response surface from sample data, and reducing the computational cost of high-fidelity code runs. It was applied to assess ECCS criteria on SiC Accident Tolerant Fuel concept. The response surface was used to estimate the cumulative risk probability due to uncertainties in ECCS performance.

References

[1] N. Siu, "Risk Assessment for Dynamic Systems: An Overview," *Reliability Engineering and System Safety*, vol. 43, pp. 43-73, 1994.

[2] D. Mandelli, A. Yilmaz, T. Aldemir, K. Metzroth and R. Denning, "Scenario Clustering and Dynamic Probabilistic Risk Assessment," *Reliability Engineering and System Safety*, vol. 115, pp. 146-160, 2013.

[3] Idaho National Laboratory, "Dynamic PRA: An Overview of New Algorithms to Generate, Analyze and Visualize Data (INL/CON-13-29508)," Idaho National Laboratory, Idaho Falls, 2013.

[4] C. Frepoli, J. P. Yurko, R. H. Szilard, C. L. Smith, R. Youngblood and H. Zhang, "10 CFR 50.46c Rulemaking: A Novel Approach in Restating the LOCA Problem for PWRs," *Nuclear Technology*, vol. 196, no. 2, pp. 187-197, 2017.

[5] Department of Energy, "Development of Light Water Reactor Fuels with Enhanced Accident Tolerance (Report to Congress)," US DOE, Washington DC, 2015.

[6] Y. Lee, "Safety of Light Water Reactor Fuel with Silicon Carbide Cladding (Doctoral Dissertation)," Department of Nuclear Science and Engineering, Masachussets Institute of Technology, Cambridge, 2013.

[7] L. I. J. Zhao, "shapeDTW: Shape Dynamic Time Warping," *Pattern Recognition*, vol. 74, pp. 171-184, 2018.

[8] H. Liu, "Taylor Kriging Metamodeling for Simulation Interpolation, Sensitivity Analysis and Optimization (Doctoral Dissertation)," Auburn University, Auburn, 2009.

[9] H. Liu, J. Shi and E. Erdem, "Prediction of Wind Speed Time Series Using Modified Taylor Kriging Method," *Energy*, vol. 35, pp. 4870-4879, 2010.

[10] D. A. Fynan and K. I. Ahn, "Implicit Treatment of Technical Specification and Thermal Hydraulic Parameter Uncertainties in Gaussian Process Model to Estimate Safety Margin," *Nuclear Engineering and Technology*, vol. 48, pp. 684-701, 2016.

[11] S. Boyd and L. Vandenberghe, Convex Optimization, Cambridge: Cambridge University Press, 2004.

[12] D. Fynan, "Uncertainty Quantification for Reactor Safety Analysis (Doctoral Dissertation)," University of Michigan, Ann Harbor, 2014.

[13] Oak Ridge National Laboratory, "Emergency Core-Cooling Systems for Light-Water-Cooled Power Reactors (ORNL-NSIC-24)," Oak Ridge National Laboratory, Oak Ridge, 1968.